Journal of Engineering Research and Applied Science
Available at www.journaleras.com
Volume 6 (2), December 2017, pp 641-651
ISSN 2147-3471 © 2017

Mineral chemistry, crystallization conditions and petrography of Cenozoic volcanic rocks in the Bahçecik (Torul/Gumushane) area, Eastern Pontides (NE Turkey)

A.Kaygusuz[1,a], Z.Merdan Tutar[2], C.Yucel[3]

[1]Gumushane University, Geological Engineering, Gumushane, Turkey.
[2]Gebze Technical University, Civil Engineering ,Kocaeli, Turkey.
[3] Gumushane University, Geological Engineering, Gumushane, Turkey.

Accepted 08 September 2017

Abstract
Mineralogical, petrographical and mineral chemistry properties are presented for the Cenozoic aged Bahçecik volcanics in the Eastern Pontides (NE Turkey). The studied volcanic rocks are composed of basaltic andesitic, andesitic, dacitic and trachydacitic lavas and pyroclastics. Petrographic and mineral chemistry studies reveal some disequilibrium textures reflecting magma mixing process. These rocks contain labradorite (An_{67-50}), andesine (An_{46-34}), oligoclase (An_{29-15}), and albite (An_{1-01}), magnesio-hastingsite (Mg# = 0.73-0.9), pargasite (Mg# = 0.76-0.78) and edenite (Mg# = 0.76-0.85), augite (Wo_{43-45}), diopside (Wo_{46}) and clinoenstatite (En_{68-69}), K-feldispar, biotite, quartz and Fe-Ti oxide minerals. Crystallization temperatures calculated from amphibole and clinopyroxene minerals are 834 °C to 1149 °C, pressure values are 1.4 to 6.5 kbar, oxygen fugacity (log10 fO_2) are -11 to -9.6. Estimation of water content calculated by using amphiboles is between 6.6 and 8.5%. Based on the obtained data, it is suggested that the magmas had undergone hydrous and anhydrous crystallizations in the shallow to mid-crustal magma chambers.

Keywords: Mineral chemistry; geothermobarometer; Cenozoic Bahçecik volcanics; eastern pontides; Torul; NE Turkey.

1. Introduction

The Eastern Pontides are characterized by three main volcanic cycles developed during Liassic, Late Cretaceous and Early Eocene to Miocene [1-3]. Although many researchers have addressed the evolution of the Cenozoic volcanic rocks in the Eastern Pontides [4-16], the studies of crystallization conditions and magma chamber processes are limited in the Bahçecik (Torul/Gümüşhane) area [17]. In this study, mineralogical, petrographical and mineral chemistry data for volcanic rocks exposed in the Bahçecik area are reported to provide thermobarometer (pressure-temperature) conditions during the crystallization and to determine settlement of the volcanics.

2. Regional geology and stratigraphy

The Eastern Pontides are commonly subdivided into the northern and southern parts (18-19). The study area is located within the northern part of the Eastern Pontides.

The basement rocks of the Eastern Pontides consist of Early Carboniferous metamorphic rocks [20] and granitoids of Late Carboniferous age [21-25]. Early and middle Jurassic volcanic and volcanoclastic rocks lie unconformably on the basement rocks, and are conformably overlain by middle–late Jurassic–Cretaceous carbonates [19, 26]. The Late Cretaceous units that unconformably overlie these carbonate rocks consist of sedimentary, volcanic and plutonic rocks. Cretaceous arc-type volcanics and intrusive rocks were emplaced into the Eastern Pontides crust [27-30]. The Lower Paleocene plagioleucitites are considered to be the final product of subduction [31]. From the Paleocene to the Early Eocene, the Eastern Pontides was above sea level probably because of the collision between the Pontides magmatic arc and the Tauride-Anatolide block [19, 32]. The

[a] Corresponding author;
Phone: +90-456-233-1000, Email: akaygusuz@gumushane.edu.tr

Eocene volcanic and volcanoclastic rocks overlie the Late Cretaceous series [8, 9, 12, 33-35], and are intruded by granitoids of similar age [36-41]. Post-Eocene uplift and erosion brought clastic input into locally developed basins [42]. In the Late Eocene, the region has remained largely above sea level with continious minor volcanism and terrigeneous sedimentation [19]. The Miocene and post-Miocene magmatisms are characterized by calc-alkaline to mildly alkaline compositions [6, 9, 43-44].

In the Bahçecik region (Figure 1), the basement rocks are consisting of Late Cretaceous dacites and pyroclastic rocks (Kızılkaya Formation, [33]). Late Cretaceous andesites and pyroclastic rocks (Çağlayan Formation, [33]) overlie these rocks conformably. Late Cretaceous Kastel Granodiorite cuts these lithologies. The Eocene sequence (Alibaba Formation, [45]), mainly of andesite, basaltic andesite with minor trachydacite and dacite and associated pyroclastics, unconformably overlie by Late Cretaceous series. Eocene volcanic rocks start with volcanic breccia, agglomerates and tuff level in the basement, and are overlain by a thick volcanic sequence including amphibole/augite andesite, quartz andesite and tuff intercalating limestone and sandstone. The top of the unit consists of dacite and their pyroclastic equivalents. The pyroclastic rocks are composed of agglomerates, tuffs and volcanics breccias.

3. Analytical techniques

Sixty-five samples were collected in the Bahçecik (Gümüşhane) area. The modal mineralogy of these samples was determined through point counting using a Swift automatic counter, and 5 representative samples being selected for electron microprobe analyses.

Electron microprobe analyses on carbon-coated polished sections were carried out at the New Mexico Institute of Mining and Technology, Socorro (USA), using a Cameca SX-100 electron microprobe with three wavelength dispersive (WD) spectrometers. Polished sections were examined using back-scattered electron imagery, and selected minerals were quantitatively analyzed. An accelerating voltage of 15 kV and a probe current of 20 nA were used. Peak count times of 20 s were used for all elements, except for F (40 s; amph/mica), F (60 s; glass), Cl (40 s), S (30 s), Sr (60 s), and Ba (60 s). A point beam of 1 □m was used for analyses of amphibole, pyroxene, epidote, Fe-Ti oxide, and zircon. A slightly defocused (10 □m) beam was used for analyses of feldspar, mica, and chlorite to avoid losses due to sodium volatilization [47].

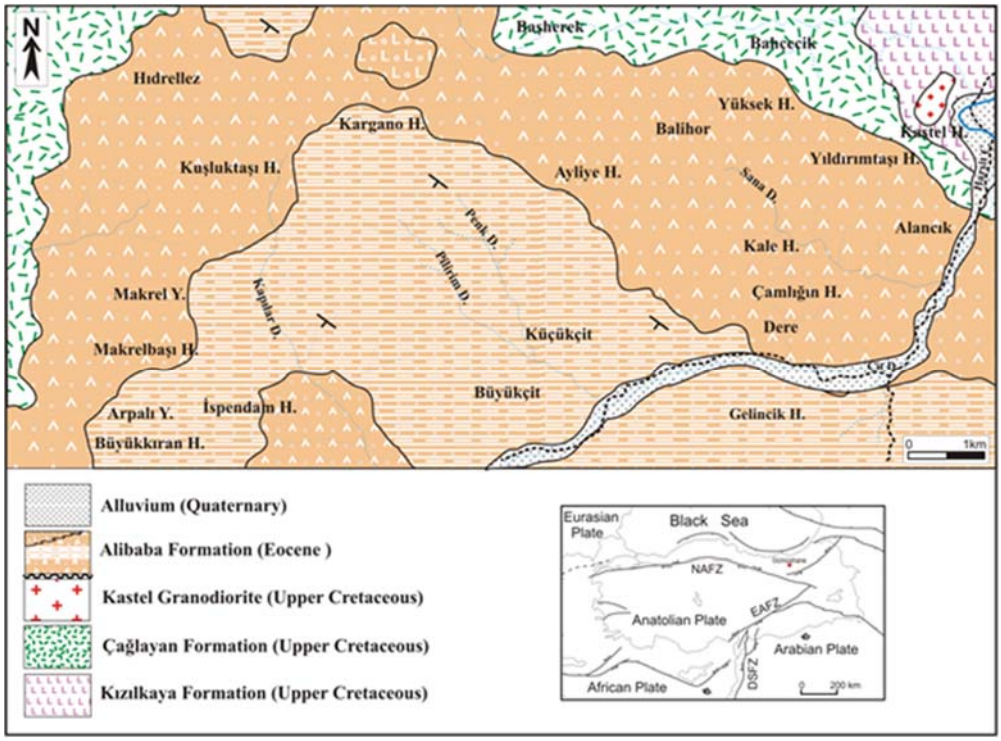

Figure 1. Geological map of the Bahçecik (Gümüşhane) area. Modified after [46].

4. Petrography and mineral chemistry

The volcanic rocks consist of basaltic andesites, andesites, minor dacites and trachydacites (Figure 2). Basaltic andesites show microlitic to microlitic–porphyric textures characterized by plagioclase, clinopyroxene and amphibole phenocrysts. Their groundmass is composed of plagioclase, clinopyroxene and amphibole microlites, and Fe–Ti oxide. Andesites have hypocrystalline porphyritic and glomeroporphyritic textures. They have phenocrysts of plagioclase, K-feldispar, ortho- and clinopyroxene and amphibole in a groundmass of microlites including plagioclase, amphibole, ortho- and clinopyroxene, and Fe–Ti oxide. Trachydacites exhibit porphyric, glomeroporphyritic and trachytic textures, including phenocrysts of plagioclase, K-feldispar, quartz, clinopyroxene and amphibole in a hyaline groundmass containing Fe–Ti oxide (Fig. 3c). Dacites exhibit holocrystalline- and microgranular textures with plagioclase, K-feldspar, quartz, amphibole and minor biotite phenocrysts. Their groundmass contains the microlites of plagioclase, amphibole, biotite, Fe–Ti oxide, and glass (Figure 2).

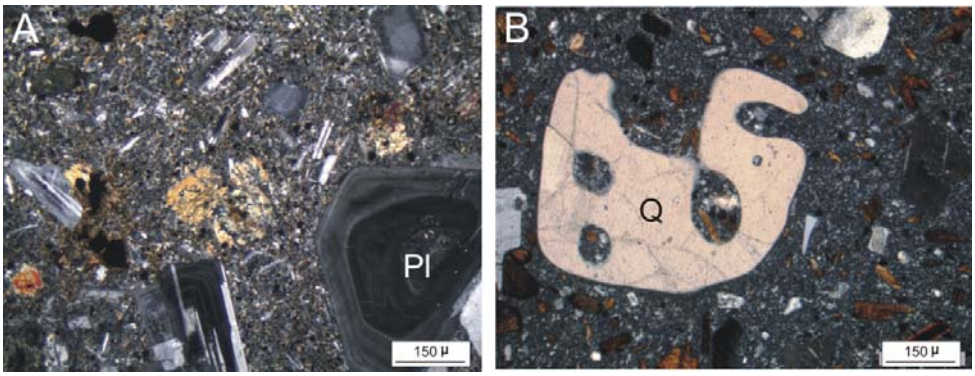

Figure 2. Photomicrography showing textural relationship of the Bahçecik volcanic rocks: (a) oscillatory zoning plagioclase; (b) embayed quartz crystals (Pl: Plagioclase, Q: Quartz) (All the microphotographs are shown in the Crossed polarized light).

The microprobe compositions for plagioclase, clinopyroxene, amphibole and Fe-Ti oxide are given in Table 1.

Plagioclase occurs as euhedral to subhedral crystals and commonly displays normal and reverse zoned. It tends to be an early, dominant phase, and some of these show oscillatory zoning (Figure 2a) and prismatic-cellular growth. Plagioclase samples show poikilitic textures, in which large plagioclase crystals may contain small crystals of plagioclase and opaque minerals. The plagioclase phenocrysts comprise broad compositions ranging from labradorite to albite ($An_{67–01}$). Anorthite composition range from An_{67} to An_{39} in basaltic andesites, from An_{46} to An_{15} in andesites, and from An_{38} to An_{01} in trachydacites (Figure 3, Table 1).

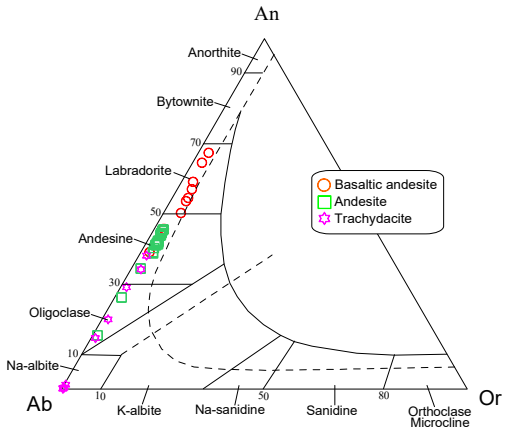

Figure 3. Classification diagram of feldspars [48].

Table 1. Minimum and maximum values of microprobe analyzes for plagioclase, pyroxene, amphibole and Fe-Ti oxide

	Plagioclase							**Pyroxene**					**Amphibole**							**Fe-Ti oxide**			
Rock types	Basaltic andesite (n=9)		Andesite (n=23)		Trachy dacite (n=10)		Rock types	Basaltic andesite (n=7)		Andesite (n=9)		Rock types	Basaltic andesite (n=4)		Andesite (n=7)		Trachy dacite (n=7)		Rock types	Basaltic andesite (n=6)		Andesite (n=6)	
	min	max	min	max	min	max		min	max	min	max		min	max	min	max	min	max		min	max	min	max
SiO2	50.42	57.56	56.44	64.03	58.12	68.09	SiO2	50.12	52.05	50.92	53.12	SiO2	42.15	44.95	44.37	46.39	45.64	46.58	SiO2	0.08	0.30	0.09	4.26
Al2O3	26.23	31.14	22.06	26.61	19.77	25.72	Al2O3	1.18	4.52	0.61	1.98	TiO2	1.09	1.32	1.06	1.44	1.09	1.34	TiO2	6.73	7.13	5.74	8.76
FeO	0.43	0.74	0.17	0.41	0.02	0.43	FeO	6.21	9.01	7.46	18.31	Al2O3	11.65	14.17	11.31	12.29	10.36	11.76	Al2O3	1.58	1.68	2.30	6.01
CaO	8.16	13.12	3.34	9.26	0.03	8.06	MnO	0.12	0.45	0.37	0.77	FeO	8.63	14.81	9.72	11.61	10.66	11.98	Cr2O3	0.00	0.05	0.05	0.08
Na2O	3.23	6.79	5.85	10.05	7.02	11.80	MgO	14.36	15.66	14.65	24.89	MnO	0.11	0.58	0.52	0.62	0.43	0.71	FeO	78.38	80.33	71.87	78.75
K2O	0.38	0.74	0.22	0.55	0.04	0.44	CaO	21.06	22.51	1.09	21.92	MgO	12.98	17.04	13.75	16.11	13.87	15.27	MnO	0.62	0.79	0.56	0.67
BaO	0.04	0.09	0.00	0.16	0.00	0.10	Na2O	0.22	0.38	0.02	0.35	CaO	11.16	11.56	10.98	12.05	10.95	11.47	MgO	0.93	1.17	1.99	2.90
Total	98.58	99.72	98.41	99.91	99.45	99.97	Total	98.04	99.81	98.22	99.14	Na2O	1.85	2.48	1.18	1.56	1.23	1.49	CaO	0.00	0.12	0.02	0.91
Si	2.32	2.59	2.57	2.84	2.62	2.98	Si	1.86	1.95	1.93	1.97	K2O	0.38	0.58	0.12	0.67	0.50	0.60	Total	88.96	91.02	91.42	92.68
Al	1.39	1.69	1.15	1.42	1.02	1.36	Ti	0.01	0.02	0.01	0.01	Total	97.97	99.15	97.02	98.92	97.19	98.88	Si	0.03	0.11	0.03	1.45
Fe2+	0.02	0.03	0.01	0.02	0.00	0.02	Al	0.05	0.20	0.03	0.09	Si	6.02	6.41	6.41	6.59	6.58	6.69	Ti	1.98	2.09	1.47	2.44
Ca	0.39	0.65	0.16	0.45	0.00	0.39	Fe2+	0.19	0.28	0.24	0.57	Ti	0.12	0.14	0.11	0.16	0.12	0.15	Al	0.72	0.78	1.00	2.42
Na	0.29	0.59	0.51	0.86	0.61	1.00	Mn	0.00	0.01	0.01	0.02	Al	1.96	2.39	1.89	2.10	1.76	2.00	Cr	0.00	0.02	0.01	0.02
K	0.02	0.04	0.01	0.03	0.00	0.03	Mg	0.81	0.87	0.83	1.38	Fe2+	1.02	1.80	1.17	1.39	1.28	1.43	Fe2+	25.69	25.98	20.52	24.21
Ba	0.00	0.00	0.00	0.00	0.00	0.00	Ca	0.84	0.90	0.04	0.89	Mn	0.01	0.07	0.06	0.08	0.05	0.09	Mn	0.20	0.26	0.16	0.21
An	39.04	67.40	15.33	45.53	0.12	38.08	Na	0.02	0.03	0.00	0.03	Mg	2.82	3.61	2.95	3.40	2.98	3.29	Mg	0.54	0.68	1.10	1.48
Ab	30.03	58.79	52.10	83.47	60.01	99.65	Wo	43.41	46.27	2.17	44.99	Ca	1.71	1.77	1.70	1.84	1.69	1.78	Ca	0.00	0.05	0.01	0.33
Or	2.16	4.32	1.20	3.23	0.23	2.51	En	41.45	43.77	41.98	69.10	Na	1.03	1.37	0.65	0.87	0.68	0.83	Fe#	0.42	0.44	0.42	0.50
Structural formula on the basis of 8 oxygen atoms							Fs	10.08	14.83	12.62	29.59	K	0.07	0.11	0.02	0.12	0.09	0.11	Structural formula on the basis of 32 oxygen atoms				
							Mg#	0.74	0.81	0.71	0.78	Mg#	0.73	0.87	0.76	0.90	0.76	0.85					
							Structural formula on the basis of 6 oxygen atoms					Structural formula on the basis of 23 oxygen atoms											

n= sample number, min: minimum values, max: maksimum values

Amphibole occurs as subhedral to euhedral phenocrystals and microlites in groundmasses. Some of larger crystals may contain small plagioclase and opaque minerals. They have $(Ca+Na)_B$ values greater than 1.00, and are calcic in composition (Figure 4a). Amphiboles from the studied rocks are classified as magnesio-hastingsite with $Al^{VI} < Fe^{3+}$ except for some pargasite with $Al^{VI} > Fe^{3+}$ and minor edenite in compositions (Figure 4b). The Mg# of amphiboles varies from 0.73 to 0.90 (Table 1). Amphibole is magnesio-hastingsite in basaltic andesite, magnesio-hastingsite to pargasite in andesite, and edenite in trachydacites (Figure 4, Table 1).

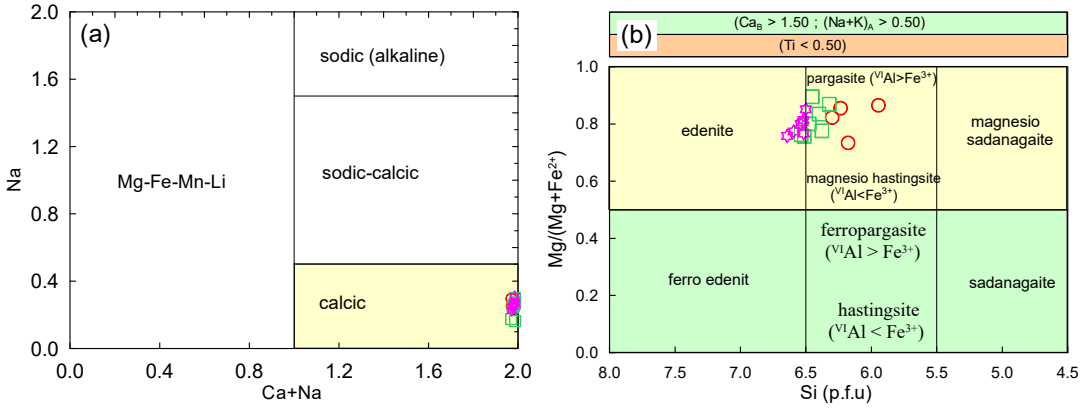

Figure 4. (a - b) The compositions of amphiboles [49]. Symbols are as in Fig. 3

Amphibole occurs as subhedral to euhedral phenocrystals and microlites in groundmasses. Some of larger crystals may contain small plagioclase and opaque minerals. They have $(Ca+Na)_B$ values greater than 1.00, and are calcic in composition (Figure 4a). Amphiboles from the studied rocks are classified as magnesio-hastingsite with $Al^{VI} < Fe^{3+}$ except for some pargasite with $Al^{VI} > Fe^{3+}$ and minor edenite in compositions (Figure 4b). The Mg# of amphiboles varies from 0.73 to 0.90 (Table 1). Amphibole is magnesio-hastingsite in basaltic andesite, magnesio-hastingsite to pargasite in andesite, and edenite in trachydacites (Figure 4, Table 1).

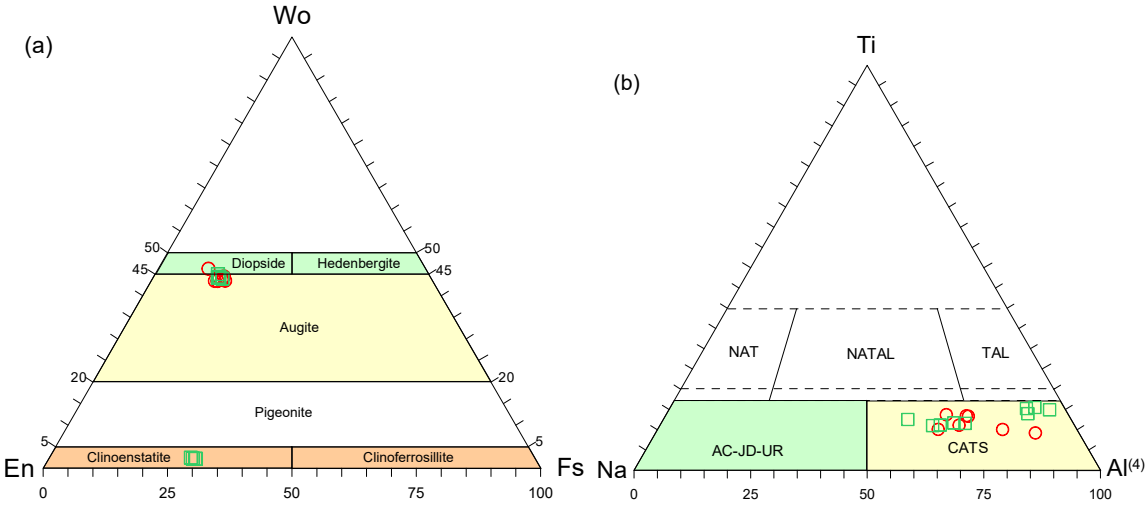

Figure 5. Classification diagrams of pyroxene, a) Wo-En-Fs [51], b) Ti-Na-$Al^{(4)}$ [50]. Symbols are as in Fig. 3

K-Feldispar is found in andesitic, trachydacitic and dacitic rocks as anhedral to subhedral microphenocryst. K–feldspar phenocrysts are sanidine and anorthoclase in compositions.

Biotite occurs only in dacitic rocks as phenocrysts and as a dispersed groundmas. Some phenocrysts may contain small plagioclase and opaque minerals.

Quartz is found only in dacitic and trachydacitic rocks. Embayed quatz crystals are common (Figure 2b).

Fe–Ti oxides are euhedral to anhedral in shape, and are in many cases adjacent to plagioclase or pyroxene phenocrysts. They are the product of the ulvospinel-magnetite solid solution and show compositions close to the magnetite in the ternary TiO_2-FeO-Fe_2O_3 diagram [52] (Figure 6).

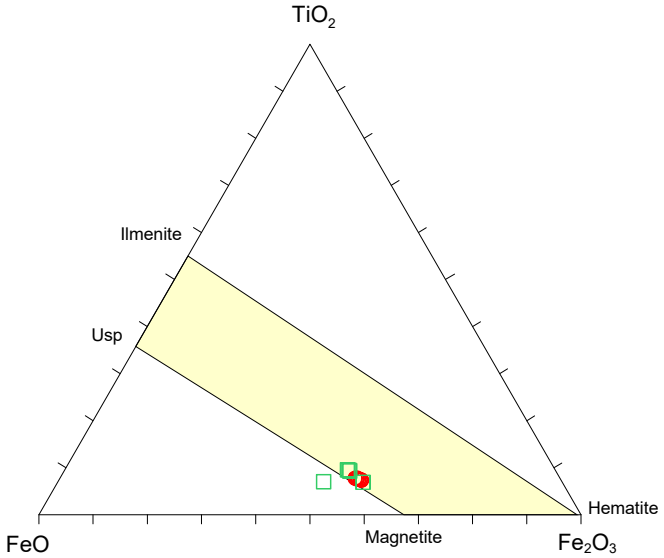

Figure 6. Plot of Fe-Ti oxides in the ternary TiO_2-FeO-Fe_2O_3 diagram [52]. Symbols are as in Fig. 3

5. Intensive parameters

5.1. Clinopyroxene thermobarometry

Estimates of quantitative temperature and pressure on clinopyroxene composition were re-evaluated by [53]. [53] gave an equilibrium constant using Fe–Mg exchange and $K_D(Fe\text{-}Mg)^{cpx\text{-}melts} = 0.27 \pm 0.03$. The calculated results of the studied rocks show pressures ranging from 1.4 to 6.3 kbar and temperatures ranging from 1081 to 1149 °C (Table 2).

Table 2. Clinopyroxene temperature and pressure calculations

Clinopyroxene-melts Thermobarometer [53]	P (32c, kbar)	T(°C)	K_D (Fe-Mg)
Basaltic andesite (n=5)			
Min	1.7	1081	0.25
Max	6.3	1149	0.27
Ort	3.8	1125	0.26
Sp	1.9	28	0.01
Andesite (n=5)			
Min	1.4	1083	0.25
Max	4.7	1123	0.26
Ort	2.5	1102	0.26
Sp	1.3	19	0.00

5.2. Amphibole-plagioclase thermobarometer

Microprobe data for the amphibole and plagioclase phenocrysts from the Bahçecik volcanites were used to calculate temperature using the equations suggested by [54]. Pressures were calculated using Al-in-amphibole method and equations proposed by [55] for volcanic rocks. The results obtained from the amphibole-plagioclase thermometer and Al-in-amphibole geobarometer are given in Table 3. Calculated pressures and temperatures give values of 3.9 to 6.5 kbar and 834 to 979 °C for the studied volcanic rocks (Table 3).

Table 3. Amphibole temperature and pressure calculations

	P (kbar) [55]	T °C [54]
Basaltic andesite (n=4)		
Min	4.7	871
Max	6.5	979
Ort	5.4	918
Sp	0.8	45
Andesite (n=7)		
Min	4.4	859
Max	5.4	902
Ort	4.9	879
Sp	0.4	16
Trachydacite (n=7)		
Min	3.9	834
Max	4.9	879
Ort	4.4	866
Sp		

5.3. Amphibole thermobarometry, oxygen fugacity, and hygrometer

[56 and 57] estimated that the P, T, H_2O contents, ΔNNO and fO_2 of volcanic rocks using microprobe analysis of amphiboles. The calculated crystallization pressures and temperatures of amphiboles in the Bahçecik volcanics were 2.3 to 4.9 kbar and 850 to 946 °C, respectively (Table 4). The relative oxygen fugacity (ΔNNO) ranged from 1.0 to 3.3 for the studied rocks (Table 4). The oxygen fugacity (log10 fO_2) values of the studied rocks varied between -9.6 and -11.0 (Table 4). Calculation results by using the formula of [56, 57] denote that the H_2O_{melt} contents of melts changed from 6.6 to 8.5 wt.% for the studied volcanic rocks (Table 4).

Table 4. Amphibole temperature, pressure, H_2O contents and oxygen fugacity calculations

			[57]				[56]	
Basaltic andesite (n=3)	T°C	P (kbar)	ΔNNO	fO_2	H_2O	P (kbar)	T°C	ΔNNO
Min	912	3.1	1.0	-10.3	6.9	3.6	907	1.6
Max	929	3.8	1.6	-10.1	7.7	4.9	942	2.0
Ort	920	3.4	1.3	-10.2	7.3	4.2	924	1.8
Sp	12	0.5	0.4	0.2	0.5	0.9	25	0.3
Andesite (n=7)								
Min	890	2.8	1.1	-10.8	6.9	3.1	890	1.7
Max	934	3.8	1.9	-9.6	8.5	4.8	946	3.3
Ort	911	3.3	1.4	-10.2	7.6	4.0	909	2.5
Sp	17	0.4	0.3	0.5	0.6	0.5	20	0.5
Trachydacite (n=7)								
Min	877	2.3	1.2	-11.0	6.6	2.7	850	1.5
Max	893	3.3	1.7	-10.4	8.1	4.3	912	2.5
Ort	884	2.8	1.4	-10.7	7.5	3.2	876	2.1
Sp	6	0.3	0.2	0.2	0.5	0.5	25	0.3

6. Discussion and Conclusions

Recent studies [34, 43, 8] suggested that the Cenozoic magmas had post-collisional characteristics and were derived from a sub-continental lithospheric mantle source that was previously modified by fluids and/or sediments. In addition, the crustal structure throughout the Eastern Pontides is not homogeneous with varying thicknesses of 29-47 km [58] and 32-40 km [59]. For this reason, the textural, petrographic and mineral chemical properties of the volcanic rocks would be changed depending on the magma chamber processes at different crustal levels.

The petrographic properties of the Bahçecik volcanics indicate that they have hydrous and anhydrous suites. The amount of water contained in the amphibole-bearing magma is controversial at rates ranging from 2 to 3 wt.% [60] to 5 wt.% [61-62] and then up to 6 wt.% [63]. The estimated H_2O_{melt} content ranges from 6.6 to 8.5 wt.% for the Bahçecik volcanic rocks (Table 4). The calculated crystallization pressures and temperatures in the studied volcanic rocks using the chemical analaysis of amphibole and orthopyroxenes are 1.4 to 6.5 kbar and 834 to 1149 °C, respectively (Table 4). The oxygen fugacity (log10 fO_2) values of the Bahçecik volcanics varied between -9.6 and -11.0 (Table 4). The combined petrographic, mineral chemistry, and thermobarometric features indicate that the magmas had undergone hydrous and anhydrous crystallizations in shallow to mid-crustal levels (~ 1 to 12 km).

Acknowledgement

This work was financially supported by the Scientific Research Projects Foundation of Gümüşhane University (Project No: 2013.F5114.02.01). Thanks are due to Ellery Frahm for microprobe analyses. An anonymous reviewer is kindly thanked for their general improvement of the manuscript.

References

[1] Çamur, M.Z., Güven, İ.H., Er, M. Geochemical characteristics of the eastern Pontide volcanics: an example of multiple volcanic cycles in arc evolution. Turkish Journal of Earth Sciences 1996; 5: 123-144.

[2] Arslan, M., Tüysüz, N., Korkmaz, S. Kurt, H. Geochemistry and petrogenesis of the eastern Pontide volcanic rocks, Northeast Turkey. Chemie der Erde 1997; 57: 157-187.

[3] Kaygusuz, A., Şen, C., Aslan, Z., Torul (Gümüşhane) volkaniklerinin petrografik ve petrolojik özellikleri (KD Türkiye); Fraksiyonel kristallenme ve magma karışımına ilişkin bulgular, Türkiye Jeoloji Bülteni 2006; 49, 1: 49–82.

[4] Tokel, S. Eocene calc-alkaline andesites and geotectonism in Black Sea Region. Geological Society of Turkey Bulletin 1977; 20: 49-54.

[5] Şen, C., Arslan, M., Van. A. Geochemical and petrological characteristics of the Pontide Eocene (?) alkaline province, NE Turkey. Turkish Journal of Earth Sciences 1998; 7: 231-239.

[6] Aydın, F., Karslı, O., Chen, B. Petrogenesis of the Neogene alkaline volcanics with implications for post-collisional lithospheric thinning of the Eastern Pontides, NE Turkey. Lithos 2008; 104: 249-266.

[7] Kaygusuz, A., K/Ar ages and geochemistry of the post-collisional volcanic rocks in the Ilıca (Erzurum) area, eastern Turkey. Neues Jahrbuch Für Mineralogie 2009; 186/1: 21-36.

[8] Arslan M., Temizel İ., Abdioğlu E., Kolaylı H., Yücel C., Boztuğ, D., Şen, C. ^{40}Ar-^{39}Ar Dating, Whole-Rock and Sr-Nd-Pb Isotope geochemistry of post-collisional Eocene volcanic rocks in the southern part of the Eastern Pontides (NE Turkey): Implications for magma evolution in extension-induced origin, Contributions to Mineralogy and Petrology 2013; 166: 113-142.

[9] Aslan, Z., Arslan, M., Temizel, İ., Kaygusuz, A., K-Ar dating, whole-rock and Sr-Nd isotope geochemistry of calc-alkaline volcanic rocks around the Gümüşhane area: implications for post-collisional volcanism in the Eastern Pontides, Northeast Turkey. Mineralogy and Petrology 2014; 108: 254-267.

[10] Temizel, İ., Arslan, M. Mineral chemistry and petrochemistry of post-collisional Tertiary mafic to felsic cogenetic volcanics in the Ulubey (Ordu) area, eastern Pontides, NE Turkey. Turkish Journal of Earth Sciences 2009; 18: 29-53.

[11] Temizel, İ., Arslan, M., Abdioğlu, E., Yücel, C. Mineral chemistry and thermobarometry of Eocene monzogabbroic stocks from the Bafra (Samsun) area in Turkey: Implications for disequilibrium crystallization and emplacement conditions, International Geology Review 2014; (56-10): 1226-1245.

[12] Eyuboğlu, Y., Dudas, F.O., Santosh, M., Yi, K., Kwon, S., Akaryalı, E. Petrogenesis and U-Pb zircon chronology of adakitic porphyries within the Kop ultramafic massif (Eastern Pontides Orogenic Belt, NE Turkey). Gondwana Research 2013; 24 (2): 742-766.

[13] Aydınçakır, E. The Petrogenesis of Early Eocene non-adakitic volcanism in NE Turkey: Constraints on the geodynamic implications, Lithos 2014; 208-209: 361-377.

[14] Kaygusuz, A., Şahin, K., Petrographical, geochemical and petrological characteristics of Eocene volcanic rocks in the Mescitli area, Eastern Pontides (NE Turkey), Journal of Engineering Research and Applied Science 2016; 5 (2): 473-486.

[15] Yücel, C., Arslan, M., Temizel, İ., Abdioğlu Yazar, E., Ruffet, G., Evolution of K-rich magmas derived from a net veined lithospheric mantle in an ongoing extensional setting: Geochronology and geochemistry of Eocene and Miocene volcanic rocks from Eastern Pontides (Turkey). Gondwana Research 2017; 45: 65-86.

[16] Gücer, M.A., Aydınçakır, E., Yücel, C., Akaryalı, E., Tersiyer yaşlı altınpınar hornblendli andezitlerinin (Torul-Gümüşhane) petrografisi, mineral kimyası ve P-T kristalleşme koşulları, Gümüşhane Üniversitesi, Fen Bilimleri Enstitüsü Dergisi 2017; 7 (2): 236-267.

[17] Kaygusuz A., Merdan Tutar., Z., Bahçecik (Torul/Gümüşhane) ve civarındaki Eosen yaşlı volkanik kayaçların petrografik, jeokimyasal ve petrolojik özelliklerinin incelenmesi. GÜ Araştırma Fonu: 2015, Proje No: 15.F5114.02.01.

[18] Özsayar, T., Pelin, S., Gedikoğlu, A., Doğu Pontidler'de Kretase. KTÜ Yer Bilimleri Dergisi 1981; 1: 65–14.

[19] Okay, A.I., Şahintürk, Ö., Yakar, H. Stratigraphy and tectonics of the Pulur (Bayburt) Region in the Eastern Pontides, Mineral Research Exploration Bulletin 1997; 119: 1-24.

[20] Topuz, G., Altherr, R., Satir, M., Schwarz, W.H., Low-grade metamorphic rocks from the Pulur complex, NE Turkey: implications for the pre-Liassic evolution of the Eastern Pontides. International Journal of Earth Sciences 2004; 93: 72–91.

[21] Yılmaz, Y., Petrology and structure of the Gümüshene Granite and surraunding rocks, North-Eastern Anatolia. PhD Thesis, University of London, 1972; 260 pp.

[22] Çoğulu, E. Gümüşhane ve Rize bölgelerinde petrografik ve jeokronolojik araştırmalar. İTÜ Kütüphanesi 1975; 1034, İstanbul.

[23] Topuz, G., Altherr, R., Wolfgang, S., Schwarz, W.H., Zack, T., Hasanözbek, A., Mathias, B,. Satır, M., Şen, C. Carboniferous high-potassium I-type granitoid magmatism in the Eastern Pontides: The Gümüşhane Pluton (NE Turkey), Lithos 2010; 116: 92-110.

[24] Dokuz, A. A slab Detachment and delamination model for the generation of Carboniferous high-potassium i-type magmatism in the Eastern Pontides, NE Turkey: Köse Composite Pluton, Godwana Research 2011; 19: 926-944.

[25] Kaygusuz, A., Arslan, M., Sipahi, F., Temizel, İ., U-Pb zircon chronology and petrogenesis of Carboniferous plutons in the northern part of the Eastern Pontides, NE Turkey: Constraints for Paleozoic magmatism and geodynamic evolution. Gondwana Research 2016; 39: 327-346.

[26] Saydam Eker, Ç., Sipahi, F., Kaygusuz, A., Trace and rare earth elements as indicators of provenance and depositional environments of Lias cherts in Gumushane, NE Turkey. Chemie der Erde Geochemistry 2012;72: 167-177.

[27] Köprübaşı, N. Şen, C., Kaygusuz, A, Doğu Pontid adayayı granitoyidlerinin karşılaştırılmalı petrografik ve kimyasal özellikleri, KD Türkiye. Uygulamalı Yerbilimleri Dergisi 2000; 1: 111–120.

[28] Karslı, O., Dokuz, A., Uysal, İ., Aydın, F., Kandemir, R., Wijbrans, J.R. Generation of the Early Cenozoic adakitic volcanism by partial melting of mafic lower crust, eastern Turkey: Implication for crustal thickening to delamination, Lithos 2010; 114: 109-120.

[29] Kaygusuz, A., Aydınçakır, E., Mineralogy, whole-rock and Sr-Nd isotope geochemistry of mafic microgranular enclaves in Cretaceous Dağbaşı granitoids, Eastern Pontides, NE Turkey: evidence of magma mixing, mingling, and chemical equilibration. Chemie der Erde Geochemistry 2009; 69: 247-277.

[30] Sipahi, F., Akpınar, İ., Saydam Eker, Ç., Kaygusuz, A., Vural, A., Yılmaz, M., Formation of the Eğrikar (Gümüşhane) Fe–Cu skarn type mineralization in NE Turkey: U–Pb zircon age, lithogeochemistry, mineral chemistry, fluid inclusion, and O-H-C-S isotopic compositions. Journal of Geochemical Exploration 2017; 182: 32-52.

[31] Altherr, R., Topuz, G., Siebel, W., Şen, C., Meyer, H.P., Satır, M., Lahaye, Y. Geochemical and Sr-Nd-Pb isotopic characteristics of Paleocene plagioleucitites from the eastern Pontides (NE Turkey). Lithos 2008; 105: 149-161.

[32] Boztuğ, D., Jonckheere, R., Wagner, G.A., Yeğingil, Z. Slow Senonian and fast Palaeocene-Early Eocene uplift of the granitoids in the Central eastern Pontides, Turkey: apatite fission-track results.

Tectonophysics 2004; 382: 213-228.
[33] Güven, G.H., Doğu Pontidlerin Jeolojisi ve 1/250000 ölçekli kompilasyonu. MTA Genel Müdürlüğü, Ankara 1993 (unpublished).
[34] Kaygusuz, A., Arslan, M., Siebel, W., Şen, C., Geochemical and Sr-Nd isotopic characteristics of post-collisional calc-alkaline volcanics in the Eastern Pontides (NE Turkey). Turkish Journal of Earth Sciences 2011; 20: 137-159.
[35] Aydınçakır, E., Şen, C. Petrogenesis of the post-collisional volcanic rocks from the Borçka (Artvin) area: Implications for the evolution of the Eocene magmatism in the Eastern Pontides (NE Turkey), Lithos 2013; (172-173): 98-117.
[36] Yılmaz, S., Boztuğ, D., Space and time relations of three plutonic phases in the Eastern Pontides (Turkey). International Geology Review 1996; 38: 935–956.
[37] Topuz, G., Alther, R., Schwarz, W.H., Siebel, W., Satır, M., Dokuz, A. Post-collisional plutonism with adakite-like signatures: the Eocene Saraycık granodiorite (eastern Pontides, Turkey). Contributions to Mineralogy and Petrology 2005; 150: 441-455.
[38] Arslan, M., Aslan, Z. Mineralogy, petrography and whole-rock geochemistry of the Tertiary granitic intrusions in the eastern Pontides, Turkey. Journal of Asian Earth Sciences 2006; 27: 177-193.
[39] Karslı, O., Chen, B., Aydın, F., Şen, C., Geochemical and Sr-Nd-Pb isotopic compositions of the Eocene Dölek and Sarıçiçek plutons, Eastern Turkey: Implications for magma interaction in the genesis of high-K calc-alkaline granitoids in a post-collision extensional setting. Lithos 2007; 98: 67–96.
[40] Kaygusuz, A., Öztürk, M., Geochronology, geochemistry, and petrogenesis of the Eocene Bayburt intrusions, Eastern Pontide, NE Turkey: implications for lithospheric mantle and lower crustal sources in the high-K calc-alkaline magmatism. Journal of Asian Earth Sciences 2015; 108: 97-116.
[41] Eyuboğlu, Y., Dudas, F.O., Thorkelson, D., Zhu, D.C., Liu, Z., Chatterjee, N., Yi, K., Santosh, M., Eocene granitoids of northern Turkey: Polybaric magmatism in an evolving arc–slab window system, Gondwana Research 2017; 50: 311-345.
[42] Korkmaz, S., Tüysüz, N., Er, M., Musaoğlu, A., Keskin, İ., Stratigraphy of Eastern Pontides, NE Turkey. In: Erler, A., et al. (Eds.), Geology of Black Sea Region Proce. of the Inter. Symp. On the Geology of Black Sea Region. MTA, Ankara 1995: 59–66.
[43] Temizel, İ., Arslan, M., Ruffet, G., Peucat, J.J. Petrochemistry, geochronology and Sr-Nd isotopic systematic of the Tertiary collisional and post-collisional volcanic rocks from the Ulubey (Ordu) area, eastern Pontide, NE Turkey: Implications for extension-related origin and mantle source characteristics, Lithos 2012; 128: 126-147.
[44] Yücel, C., Arslan, M., Temizel, İ., Abdioğlu, E. Volcanic facies and mineral chemistry of Tertiary volcanics in the northern part of the Eastern Pontides, northeast Turkey: Implications for pre-eruptive crystallization conditions and magma chamber processes, Mineralogy and Petrology 2014; 108: 439-467.
[45] Tokel, S., Stratigraphical and volcanic history of the Gümüşhane region (NE Turkey), Ph. D. Thesis, University Colloge, London 1972.
[46] Merdan Tutar, Z., Bahçecik (Torul/Gümüşhane) ve civarındaki Eosen yaşlı volkanik kayaçların petrografik, jeokimyasal ve petrolojik özelliklerinin incelenmesi. Yüksek Lisans Tezi, Gümüşhane Üniversitesi, Fen Bilimleri Enstitüsü, Gümüşhane, 2015; 103s.
[47] Nielsen, C.H., Sigurdsson, H., Quantitative methods for electron microprobe analysis of sodium in natural and synthetic glasses. American Mineralogist 1981; 66: 547−552.
[48] Smith, J.V., Brown, W.L., Feldspar Minerals. Second review and extended edition Book (ISBN 0387176926), Springer-Verlag, Berlin 1988.
[49] Leake, E.B., Wooley, A.R., Arps, C.E.S., Birch, W.D., Gilbert, M.C., Grice, J.D., Hawthorne, F.C., Kato, A, Kisch, H.J., Krivovichev, V.G., Linthout, K., Laird, J., Mandarino, J., Maresch, W.V., Nickhel, E.H., Rock, N.M.S., Schumacher, J.C., Smith, D.C., Stephenson, N.C.N., Ungaretti, L., Whittaker, E.J.W. Youzhi, G., Nomenclature of amphiboles report of the subcommittee on amphiboles of the International Mineralogical Association Commission on New Minerals and Mineral Names. European Journal of Mineralogy 1997; 9: 623-651.
[50] Papike, J.J., Cameron, K.L. Baldwın, K., Amphiboles and Pyroxenes: Characterization of other than Quadrilateral Components and Estimates of Ferric Iron from Microprobe Data. Geological Society of America 1974; 6: 1053-1054.

[51] Morimoto, M., Nomenclature pyroxenes. Mineralogical Magasine 1988; 52: 535-550.
[52] Bacon C.R. Hirschmann, M.M., Mg/Mn partitioning as a test for equilibrium between coexisting Fe-Ti oxides. American Mineralogist 1988; 73: 57-61.
[53] Putirka, K.D., Thermometers and barometers for volcanic systems. In: Putirka K.D., Tepley, F., (eds). Reviews in Mineralogy 2008; 69: 61–120.
[54] Blundy, J.D., Holland, T.J.B., Calcic amphibole equilibria and a new amphibole-plagioclase geothermometer. Contributions to Mineralogy and Petrology 1990: 208–224.
[55] Johnson, M.C. Rutherford, M.J., Experimental calibration of the aluminiun-in amfibole geobarometer with application to Long Valley Caldera (California) volcanic rocks. Geology 1989; 17: 837-841.
[56] Ridolfi F., Renzulli, A., Calcic amphiboles in calc-alkaline and alkaline magmas: thermobarometric and chemometric empirical equations valid up to 1,130°C and 2.2 Gpa. Contributions to Mineralogy and Petrology 2012; 163: 877-895.
[57] Ridolfi, F., Renzulli, A., Puerini, M., Stability and chemical equilibrium of amphibole in calc-alkaline magmas: an overview, new thermobarometric formulations and application to subduction- related volcanoes. Contributions to Mineralogy and Petrology 2010; 160. 45–66.
[58] Maden, N., Gelişli, K., Eyüboğlu, Y., Bektaş, O., Two-andthree-dimensional crustal thickness of the eastern Pontides (NE Turkey). Turk J Earth Sci 2009; 18(2): 225–238.
[59] Çakır, Ö., Erduran, M., Constraining crustal and uppermost mantle structure beneath station TBZ (Trabzon, Turkey) by receiver function and dispersion analyses. Geophys J Int 2004; 158: 955–971.
[60] Luhr, J.F., Slab-derived fluids and partial melting in subduction zones: insights from two contrasting Mexican volcanoes Colima and Ceboruco. J Volcanol Geotherm Res 1992; 54: 1–18.
[61] Eggler, D.H., Water-saturated and undersaturated melting relations in a Paricutin andesite and an estimate of water content in the natural magma. Contrib Mineral Petrol 1972; 34: 261–271.
[62] Helz, R.T., Phase relations of basalts in their melting ranges at PH_2O =5 kb as a function of oxygen fugacity. J Petrol 1973; 14: 249–302.
[63] Merzbacher, C., Eggler, D.H., A magmatic geohygrometer: application to Mount St. Helens and other dacitic magmas. Geology 1984; 12: 587–590.